

# **F-Praktikum Astronomy**

Pulsar observations with the Low Frequency Array

AIRUB

December 21, 2023



**Astronomisches Institut  
RUHR-UNIVERSITÄT BOCHUM**

Supervisor: Björn Adebarh

# Contents

<b>1</b>	<b>Introduction</b>	<b>2</b>
1.1	Structure of this handbook . . . . .	2
1.2	History of pulsar discovery . . . . .	2
<b>2</b>	<b>Fundamental Physics</b>	<b>3</b>
2.1	Pulsar origin and spatial distribution . . . . .	3
2.2	Characteristics of pulsars in the radio sky . . . . .	5
2.3	Pulsar evolution . . . . .	7
2.4	Propagation effects . . . . .	8
2.4.1	Dispersion Measure (DM) . . . . .	9
2.4.2	Rotation Measure (RM) . . . . .	11
<b>3</b>	<b>Radio interferometry and the LOFAR telescope</b>	<b>13</b>
3.1	Introductory remarks . . . . .	13
3.2	The LOFAR telescope . . . . .	13
3.3	RFI . . . . .	15
<b>4</b>	<b>Choosing your targets</b>	<b>17</b>
<b>5</b>	<b>Analysis</b>	<b>18</b>
5.1	Technical advice . . . . .	18
5.2	Working with the data . . . . .	18
5.2.1	Data inspection . . . . .	18
5.2.2	Flagging . . . . .	20
5.2.3	DM correction . . . . .	21
5.2.4	Period correction . . . . .	22
5.2.5	Rotation measure correction . . . . .	23
5.3	Galactic magnetic field and distance . . . . .	26
5.4	Pulsar magnetic field and characteristic age . . . . .	27
5.5	Special effects . . . . .	27
<b>A</b>	<b>Famous pulsars</b>	<b>32</b>
<b>B</b>	<b>Remote access</b>	<b>33</b>
B.1	VPN Connection . . . . .	33
B.2	GUI-Access . . . . .	33
B.2.1	X2GOCleint . . . . .	33
B.2.2	PuTTY and X-11 forwarding . . . . .	33
<b>C</b>	<b>Linux terminal commands</b>	<b>34</b>

# 1 Introduction

## 1.1 Structure of this handbook

This lab course aims to convey the fundamental knowledge to understand the physics of pulsars. Specifically, on the technical side, you will schedule a radio observation, work with certain data-formats often used in pulsar astronomy, and as a prerequisite gain knowledge about the Low Frequency Array (LOFAR) radio telescope, as one of its stations is going to perform the observation for you. Starting with fundamental knowledge, section 2 provides useful information about pulsars and their properties. Section 3 introduces radio interferometry and places special emphasis on the LOFAR telescope.

The major tasks of this lab course can be separated into two blocks, sections 4 and 5. The first section explains how you can query a catalogue of pulsars with Python code that will be provided to you to identify candidate pulsars for your planned observations. The latter section handles the analysis of the data taken for you. This includes the investigation of important physical parameters and properties of the observed pulsars. In the end, you can use your analyzed data to estimate the strength of the interstellar magnetic field and the distance to each individual pulsar.

At the end of sections 2 and 3, *key questions*, *questions to think about* and *bonus questions* can be found. The *key questions* are intended as a reference for the review of the content. The answers to the *questions to think about* are not directly mentioned in this document. Both type of questions should be discussed in the protocol. The *bonus questions* can be used as guidelines to look deeper into the topic of pulsars.

## 1.2 History of pulsar discovery

Pulsars were first detected at the university of Cambridge, where Anthony Hewish and his students had build a new radio telescope with improved time resolution. The summary given here is based on Bell-Burnell (1977). Hewish and co-workers were aiming to identify radio-quasars (point sources in the radio sky, which are actually distant active black holes radiating in the radio regime) by their scintillation in the hot plasma of the solar corona (Wilson et al., 2013), which means that they "twinkle" in the plasma of the solar system similar to stars in the Earth's atmosphere.

Jocelyn Bell-Burnell, then a doctorate student originally from Scotland, remained with Hewish after the construction of the telescope was completed, starting her search for quasars. In addition to finding many of them, she also stumbled upon an interesting signal, which she thought was man-made. Luckily, she re-observed the same signal with higher time-resolution and found regular pulses of 1.337 s separation. While re-observing the source, it appeared periodically after one sidereal day, indicating that the source was likely to be located outside of the solar system.

While these signals were first thought to be of extraterrestrial origin, several more periodic signals were found shortly after the first detection. This made the "Little Green Men"-theory unreliable. Later several of these signals could be traced back to the centers of supernova remnants, so that neutron stars were the most likely origin. The discovery of these signals was rewarded with the Nobel Prize for Anthony Hewish in 1974.

### Bonus question

Why are pulsars scientifically so important? Which fundamental physical laws can be tested with them? Inform yourself about "pulsar timing" and the "Hulse-Taylor pulsar"!

## 2 Fundamental Physics

### 2.1 Pulsar origin and spatial distribution

Pulsars are the product of stellar evolution, i.e., they are neutron stars with special characteristics (Sec. 2.1). Neutron stars generally form in core-collapse supernovae from the imploding cores of stars with initial masses of approximately 8–25  $M_{\odot}$ . As such they are an end state of stellar evolution, being more massive than white dwarf stars and less massive than black holes. In other words, they are massive enough to overcome the electron degeneracy pressure that stabilizes white dwarfs, but not as massive as to overcome the neutron degeneracy pressure that arises when even protons and electrons fuse to form neutrons. This makes neutron star matter even denser than atomic nuclei (Lorimer & Kramer, 2004)!

The typical pulsar mass is measured to be close to  $1.4 M_{\odot}$  (Lorimer & Kramer, 2004). (Note: This is close to the Chandrasekhar mass of  $1.4 M_{\odot}$ .) Heavier pulsars with around  $2 M_{\odot}$  have also been found (e.g. Antoniadis et al., 2013). The current estimate of the maximum possible mass of a neutron star (which includes pulsars) is  $2.2 M_{\odot}$ – $2.3 M_{\odot}$  (Lattimer, 2021).

#### Key question

What is the current state of research concerning the mass range of pulsars?

Making very general assumptions about the pulsar interior and its equation of state (the pressure-density relation), the minimum radius of a pulsar can be estimated as

$$R_{\min} \simeq 1.5 R_S = \frac{3GM}{c^2} = 6.2 \text{ km} \left( \frac{M}{M_{\odot}} \right) \quad (1)$$

while the maximum radius is

$$R_{\max} \simeq 16.8 \text{ km} \left( \frac{M}{M_{\odot}} \right)^{1/3} \left( \frac{P}{\text{ms}} \right)^{2/3}, \quad (2)$$

which can be inferred by assuming that the pulsar is stable under rotation. Note that the resulting radii are very close to the Schwarzschild-radius  $R_S$  of the respective masses, implying that neutron stars are almost black holes and that the gravitational field around one must be extreme (Lorimer & Kramer, 2004).

#### Key question

How massive and how large are neutron stars approximately? How are the masses and radii of other end states of stellar evolution?

The extreme gravitational forces lead to very high pressures and densities within the interior of neutron stars. Accordingly, it is assumed that they contain several exotic matter states. Most models agree on the following internal structure (Lorimer & Kramer, 2004): at the surface, a neutron star is thought to have a solid crust consisting of mainly iron nuclei and degenerate electrons with  $\rho \simeq 10^6 \text{ g cm}^{-3}$ . Further inward, a nucleon-rich core will be formed as protons and electrons are fused to neutrons. Having reached the density of  $\rho \simeq 4 \times 10^{11} \text{ g cm}^{-3}$ , the number of neutrons released from the nuclei will increase quickly, until all nuclei dissolve in a neutron superfluid mixed with  $\sim 5\%$  electrons and protons, which forms the largest fraction of the neutron star. The (estimated) average density of neutron stars is around  $\rho_{\text{avg}} \simeq 6.7 \times 10^{14} \text{ g cm}^{-3}$ , while for atomic nuclei it is only  $\rho_{\text{nuc}} \simeq 2.7 \times 10^{14} \text{ g cm}^{-3}$  (Lorimer & Kramer, 2004). An illustration of the structure is given in Figure 1.

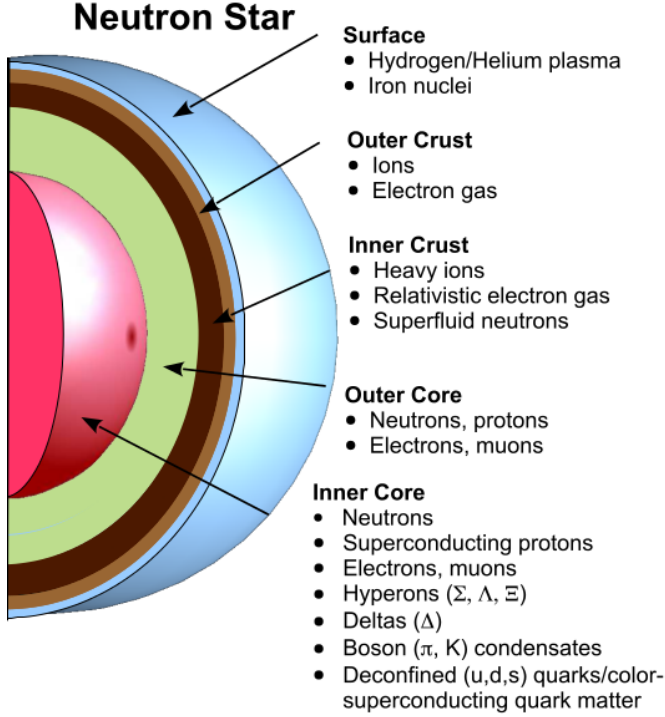


Figure 1: Schematic illustration of the internal structure of a neutron star. The list labeled as "inner core" contains several hypotheses what kind of matter might be present in the center, which is by no means clear. Illustration available from <https://astrobites.org/wp-content/uploads/2014/08/quark-neutronstar.png>

Pulsars generally exhibit a fast rotation and have a strong magnetic field. These properties are essential for the pulsed radio emission. While the origin of the rotation is not entirely clear, it is assumed that pulsars are "kicked" while they are born, because supernova explosions can happen slightly asymmetrically. The strength of the magnetic field can be explained as follows. The neutron matter of the pulsar is superconductive, which "freezes" the magnetic field lines and conserves magnetic flux. This way, the magnetic field of the star is virtually compressed to the size of the pulsar, making it many orders of magnitude stronger. The typical magnetic field strength of a pulsar is estimated to be around  $10^{11}$ - $10^{12}$  G. However, the actual range is larger, covering  $10^7$ - $10^{14}$  G at the surface of the pulsar (ATNF Pulsar Catalogue, 2022).

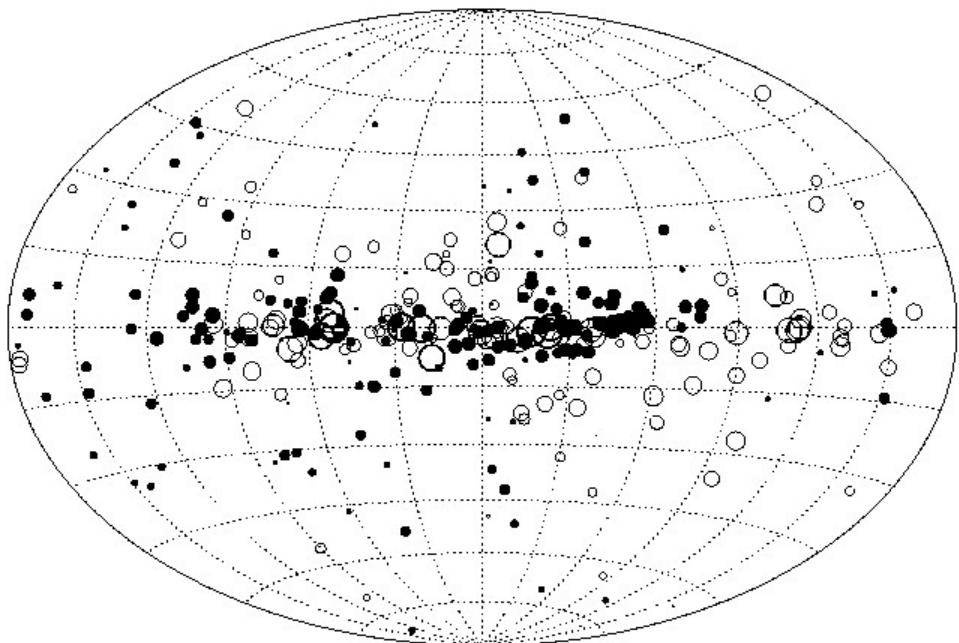
As of August 2022, there are 3320 pulsars listed in the Pulsar Catalogue of the Australian Telescope National Facility (ATNF), which lists basically all confirmed pulsars (Manchester et al., 2005; ATNF Pulsar Catalogue, 2022). 662 pulsars have periods less than 100 ms, and for 467 pulsars of them it is less than 10 ms (ATNF Pulsar Catalogue, 2022), making them "millisecond pulsars". As of now, radio pulsars have only been detected in the Milky Way including the globular clusters in its halo. Pulsating sources in  $\gamma$ - and X-rays, presumably neutron stars as well, have also been found extragalactic, e.g., in the Large Magellanic Cloud (The Fermi LAT Collaboration, 2015) and the Andromeda Galaxy (Zolotukhin et al., 2016).

In the disk of the Milky Way, the two dimensional spatial pulsar density declines radially outwards from the center. At 4 kpc distance from the galactic center it reaches about 200 pulsars/kpc<sup>2</sup>, while in the solar neighborhood (8 kpc from the center), this decreases to  $30 \pm 6$  pulsars/kpc<sup>2</sup> and even further out at 12 kpc to 10 – 15 pulsars/kpc<sup>2</sup> (Wilson et al., 2013). The distribution of pulsars in z-direction (above and below the galactic plane) is more peculiar: the pulsars roughly follow an exponential density distribution with a scale height of 600 pc. This is significantly larger than the scale height of any other class of objects related

to their progenitor stars, excluding objects in globular clusters. Possible explanations arise when looking at the velocity distribution of various pulsars: transverse velocities of 100 – 200 km/s are common and total velocities reaching  $\sim$ 450 km/s can frequently be detected (Wilson et al., 2013). Hence, many pulsars are fast enough to escape the gravitational potential of the galaxy, explaining why they can be found substantially further outward than their progenitors.

### Key question

How are pulsars distributed in the galaxy? How can the distribution be explained qualitatively?



Taken from "Handbook of Pulsar Astronomy" by Lorimer & Kramer

Figure 2: Plot of the height distribution above the galactic disk of a pulsar sample. The galactic center is in the center of the projection. Taken from Lorimer & Kramer (2004).

Mapping the distribution of pulsars in space requires knowing their position on the sky, but also their distance. There are several methods for measuring the distances of pulsars, which all have advantages and disadvantages. One of them will be introduced and used in this lab course.

### Bonus question

Which techniques can be used to measure the approximate distance to pulsars?

## 2.2 Characteristics of pulsars in the radio sky

A general observational characteristic that makes a neutron star a pulsar is re-occurring periodic radio emission. So far, the origin of this pulsed radio signal is not fully understood. However, the periodicity of the radio emission can be traced back to the misalignment of the rotation axis in comparison to the magnetic axis of a pulsar. Three types of pulsars are distinguishable by their prime energy generation mechanism: rotation-powered, accretion-powered, and magnetically powered pulsars. The first one represents by far the largest class of pulsars. Rotation-powered pulsars convert their rotational energy into electromagnetic radiation and slow down in the process, while, e.g., accretion-powered pulsars gain additional energy from the accretion of matter from a binary partner.

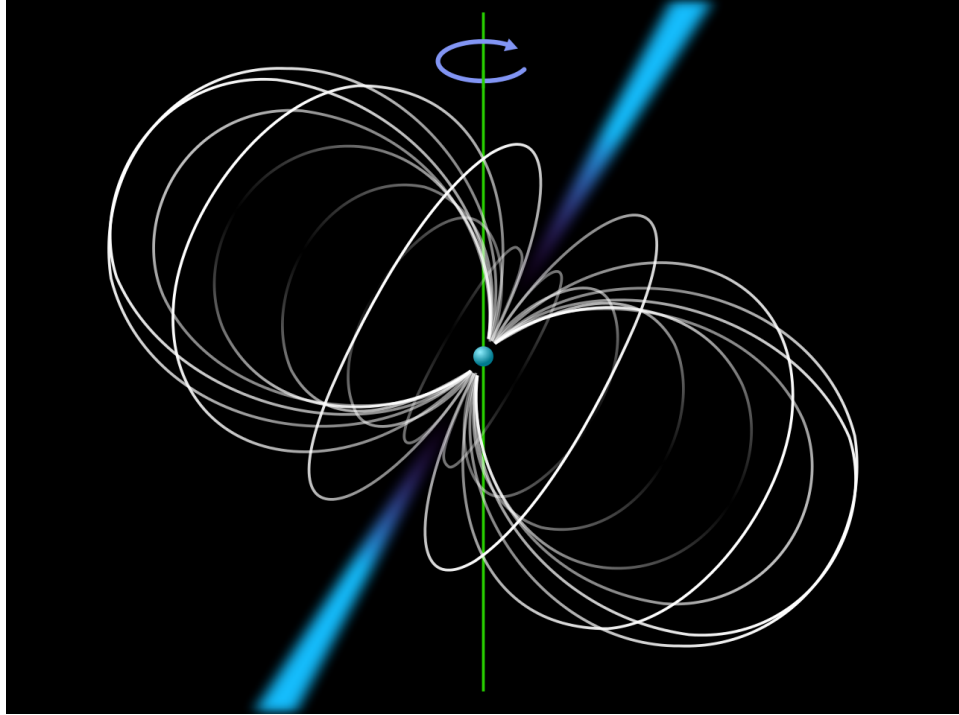


Figure 3: Schematic illustration of the magnetic field (white lines), the radio beam that is aligned with it (blue), and the axis of rotation (green).

The formerly mentioned misalignment of the rotational and magnetic axes, whose orientations are both assumed to be constant over a long period of a pulsar’s lifetime, causes the stable pulsed signal. The magnetic field of the a pulsar has the form of a magnetic dipole, where the field lines closest to the magnetic poles are parallel to the magnetic axis. Since the matter in neutron stars is superconducting, the magnetic field lines are frozen to their surface. Therefore the magnetic field lines do not intertwine, despite the neutron stars’ fast rotation.

The electrons gyrate around the magnetic field lines and emit synchrotron radiation continuously. Due to the relativistic motion of the electrons along the magnetic field lines, their radio emission is beamed in the direction of the field lines. These characteristics of a pulsar can be summarized in a lighthouse-model shown in Figure 3. The radio emission of a pulsar generally has the following characteristics that we make use of later in the analysis: **a)** a non-thermal power-law spectrum  $S \sim f^{-\alpha}$  with  $\alpha$  often about 1.6, **b)** the emission is originating from a point-like source region, and **(c)** the emission is polarized. The beamed radio emission generally sweeps over the observer depending on the rotational period of the pulsar causing its typical pulse profile.

Each observed single pulse looks slightly different. Due to the faintness of these pulses, we usually add around 100 to 1000 pulses up to determine an average intensity profile, see Sec. 2.4). This profile is found to be remarkably stable over time but individual for every pulsar (Lorimer & Kramer, 2004). The average intensity profile is also known as the fingerprint of a pulsar and generally referred to when classifying the source. Different pulse profiles can be seen in Figure 4. The shape of the profile can depend on the different classes of pulsars as well as the offset between the beam and the rotational axis of the neutron star. They typically show one major peak which corresponds to the center of the beam passing over the line-of-sight (LOS). The shape and strength of minor subpeaks depend on the inclination of the observer to the rotation-axis, the state of the pulsar and the environment it is situated in.

### Key question

What are the special characteristics of pulsars as a type of radio source? Why do we observe the radio emission as pulsed?

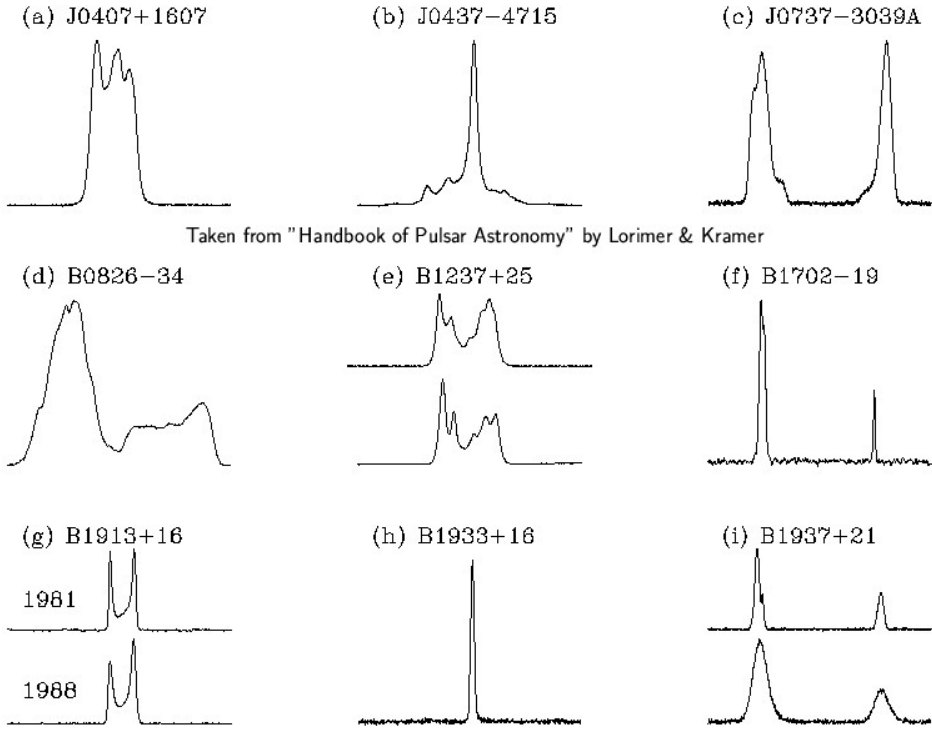


Figure 4: Integrated pulse profiles of different pulsars, demonstrating the variation among the population. For B1937+21, two techniques (with different precision) to correct for the dispersion effects in the ISM were employed. The upper profile is the correct one. From Lorimer & Kramer (2004).

### 2.3 Pulsar evolution

The evolution of a pulsar and corresponding characteristics can be shown in a so called  $P\dot{P}$ -diagram. These are two parameters of a pulsar that can directly be measured: the rotation period  $P$  and its derivative  $\dot{P}$  (pronounced as "P dot"). While reducing the data to the pulse profile (see sec. 5.2, 5.2.1) the averaged period of the pulsar can be gained. To measure the period derivative, successive observations of the pulsar are needed. This derivative can be translated to the energy loss through a model of a magnetic-dipole rotation-powered pulsar. This model can be used to determine the lower limit of the magnetic field strength  $B$  at the surface of the pulsar and the *characteristic age*  $\tau$  via  $P$  and  $\dot{P}$ .  $\tau$  approximates the time the pulsar has been radiating assuming that its magnetic field did not change. These characteristics can be assigned to certain regions, i.e. lines of constant  $B$  or constant  $\tau$ , in the  $P\dot{P}$ -diagram.

The derivation starts with the radiation power of a magnetic dipole  $P_{\text{rad}}$  that is changing its orientation through rotation around an axis. For a uniform rotation, this only depends on the magnetic moment  $m$  of the dipole and the period  $P$ .  $m$  can be approximated as that of a magnetized sphere, which introduces the magnetic field strength  $B$  and the radius of the pulsar  $R$ .  $P_{\text{rad}}$  can be expressed in terms of  $P$  and  $\dot{P}$  to obtain a relation for  $B$ :

$$B > \left( \frac{3cI}{8\pi^2 R^6} \right)^{1/2} (P\dot{P})^{1/2}, \quad (3)$$

with  $I$  being the moment of inertia of a spherical neutron star. To draw lines of constant  $B$  into the  $P\dot{P}$ -diagram one has to assume values for  $I$  and  $R$ . Fortunately, the mass and the radius are relatively constant

for most pulsars in comparison to  $P$  and  $\dot{P}$ . Thus, only  $P$  and  $\dot{P}$  have a significant influence on the position of the lines of constant  $B$ .

Assuming  $B$  to be constant, the product  $P\dot{P}$  (see Eq. 3) is constant over the lifetime of the pulsar. By integration over the lifetime of the pulsar and its period since birth  $P_0$

$$\int_{P_0}^P P dP = \int_0^\tau P \dot{P} dt \quad (4)$$

$$= P \dot{P} \int_0^\tau dt \quad (5)$$

$$\longrightarrow \frac{1}{2}(P^2 - P_0^2) = P \dot{P} \tau \quad (6)$$

one can determine the characteristic age  $\tau$  as

$$\tau = 2 \frac{P}{\dot{P}}. \quad (7)$$

### Key question

What is the  $P\dot{P}$ -diagram? Why can one draw lines of constant magnetic field strengths and characteristic ages into it?

An example of a  $P\dot{P}$ -diagram with the corresponding lines of constant  $B$  and  $\tau$  is given in Fig. 5.

### Question to think about

How would a pulsar that is only powered by rotation (like in the model discussed above) move in the  $P\dot{P}$  diagram during its lifetime? Study the diagram more closely or do some research on your own. To what extent is this scenario supported by observation?

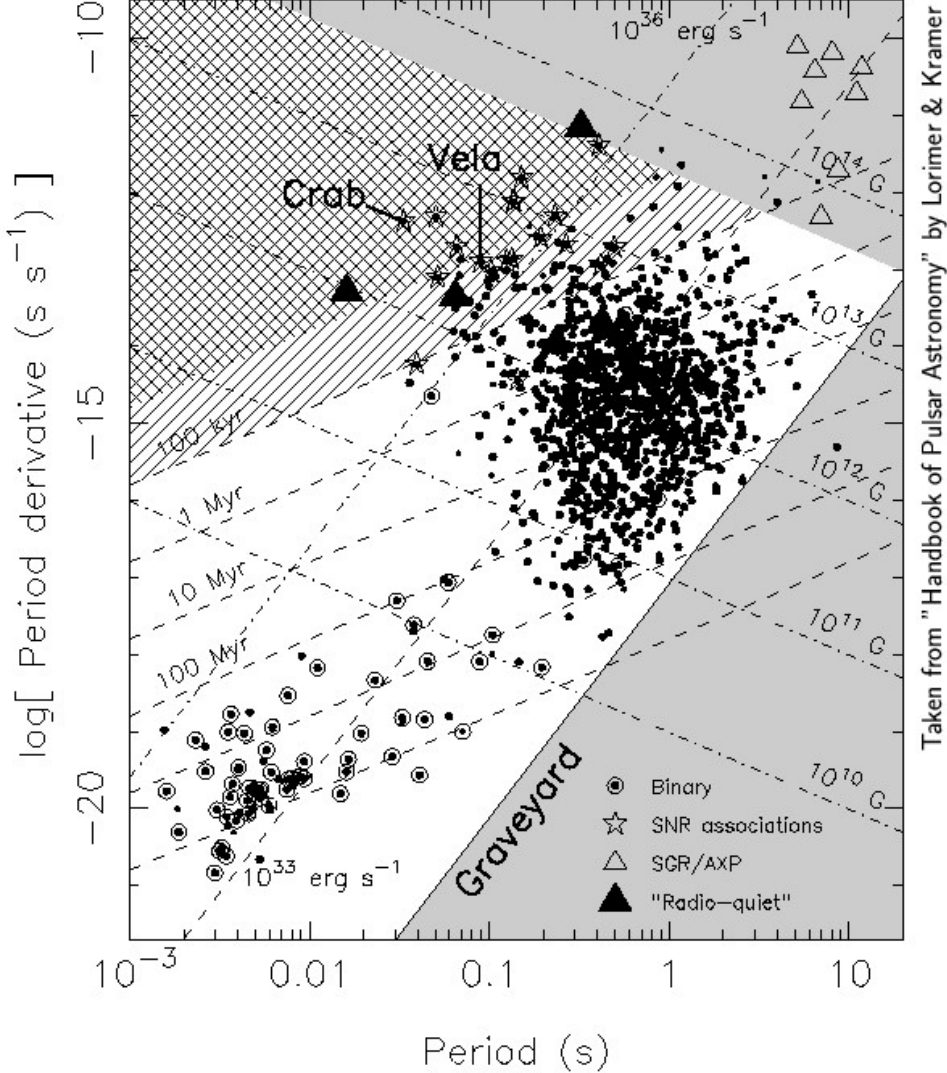
This diagram is useful to discriminate between two distinct populations of pulsars. One population consists of pulsars with a period of about (0.1-5) s, with some of the youngest ones still associated with supernova remnants. The other population shows periods in the range of (0.001-0.1) s and has a lower fraction of observed pulsars than in the first population. These are the so called *millisecond pulsars*. The differences in  $P$  and  $\dot{P}$  between the two populations suggest that the main process governing their evolution is not the same. This is supported by the fact that most millisecond pulsars are found in binary systems suggesting that they have gone through an accretion-powered process, which is also known as *recycling*.

### Question to think about

Where in the galaxy do you expect the density of millisecond pulsars to be especially high?

## 2.4 Propagation effects

The pulsar signal will be altered by the magnetic fields and charged particles in the interstellar medium during its propagation along the LOS. The primary distorting effects are called *dispersion* and *Faraday rotation*. Dispersion refers to a frequency-dependent delay due to the free-electron plasma along the LOS. Faraday rotation is a change in orientation of the polarization vector, which is caused by the free electrons in combination with a magnetic field parallel to the LOS. The corresponding observables are called *dispersion measure* (DM) and the *rotation measure* (RM), respectively. These quantities will be measured and corrected for during the data analysis for this lab course.



Taken from "Handbook of Pulsar Astronomy" by Lorimer & Kramer

Figure 5: Example of a  $P-\dot{P}$ -diagram from Lorimer & Kramer (2004). One can clearly see the distinct populations of regular and millisecond pulsars. The grey area or "graveyard" is a region where radio pulsars are not supposed to exist according to most theoretical models. Also note the lines of equal characteristic age (dashed from bottom left to top right, in kyr or Myr), equal magnetic field strength (dashed-dotted from top left to bottom right, in G) and equal radiated power (dashed-dotted from bottom left to top right, in erg/s).

#### 2.4.1 Dispersion Measure (DM)

Dispersion refers to different velocities of radio waves depending on their frequencies. Note that modern radio telescopes generally measure the signal of radio emission in several individual frequency channels over a certain bandwidth (see Sec. 3 for more details). Thus, dispersion causes the pulses in different frequency channels to be delayed with respect to one another. This delay is proportional to the inverse of the frequency squared, which means that radio waves with lower frequencies are delayed more than those with higher frequencies. Additionally, an increased number density of electrons  $n_e$  also delays a radio signal. Hence, the total amount of delay corresponds to the integrated column density of the electrons along the LOS, the DM. For practical observations, the delay between two frequency channels can be expressed as

$$\Delta t \simeq 4.15 \times 10^6 \text{ ms} \times \left( \frac{1}{f_{\text{ref}}^2} - \frac{1}{f_{\text{chan}}^2} \right) \times \text{DM}, \quad \text{where } \text{DM} = \int_0^d n_e \, dl, \quad (8)$$

where  $d$  is the distance to the pulsar. DM is usually given in units of  $\text{cm}^{-3} \text{ pc}$ . To analyze a pulsar signal, the delay has to be compensated for. This is often done based on an optimal fit of DM that maximizes, i.e., the signal-to-noise ratio (SNR) of the pulse profile.

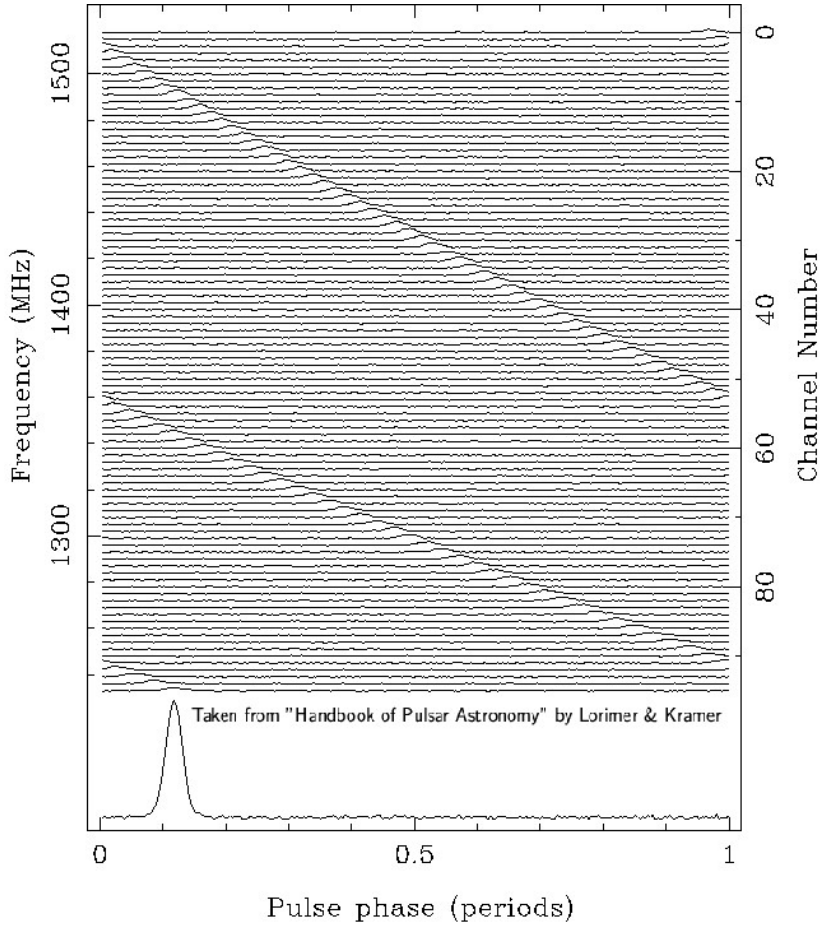


Figure 6: Diagram showing the folded pulse profiles of many frequency channels in an observation of B136-60 (period 128 ms) by the Parkes radio telescope. The fact that the pulses come at different times in different channels is due to dispersion in the ISM. From Lorimer & Kramer (2004).

You can visualize the process by thinking of time-resolved radio signals in different frequency channels that have to be shifted so that the pulses overlay correctly. This is known as *incoherent de-dispersion*, where only the time stamps of different frequency channels are adjusted. In addition, there is a more precise method called *coherent de-dispersion*, in which the radio data is processed in a more sophisticated way. Fortunately, the pulsar software will perform the de-dispersion largely automatically. Figure 6 shows a pulse phase vs. frequency diagram in which you can see the effects of the dispersion-induced delay.

#### Key question

Why do different frequency bands experience a constant relative delay? Does this delay depend on the pulsar? Why is it important for pulsars, but not for most other radio sources? How and why do we compensate for it?

#### Question to think about

What would change in Fig. 6 if the dispersion was properly corrected for? In other words, how would a pulse phase vs. frequency diagram look if the radio signal was not dispersed?

### 2.4.2 Rotation Measure (RM)

The *Faraday effect* causes the rotation of the polarization vector of a radio wave in the presence of a magnetic plasma with non-zero LOS component. Note that the rotation, that a pulsar signal experiences, is mainly due to the magnetic field within the Milky Way's interstellar medium. The magnetic field of the pulsar has no significant effect, since its spatial extent is very limited. The RM corresponds to the total amount of rotation a polarization vector is subjected to during propagation. It is proportional to an integral over the magnetic field strength along the LOS  $B_{\parallel}$  and the electron number density (see Eq. 9). The change in the polarization angle  $\Psi_{PA}$  depends on the frequency squared and is proportional to RM.

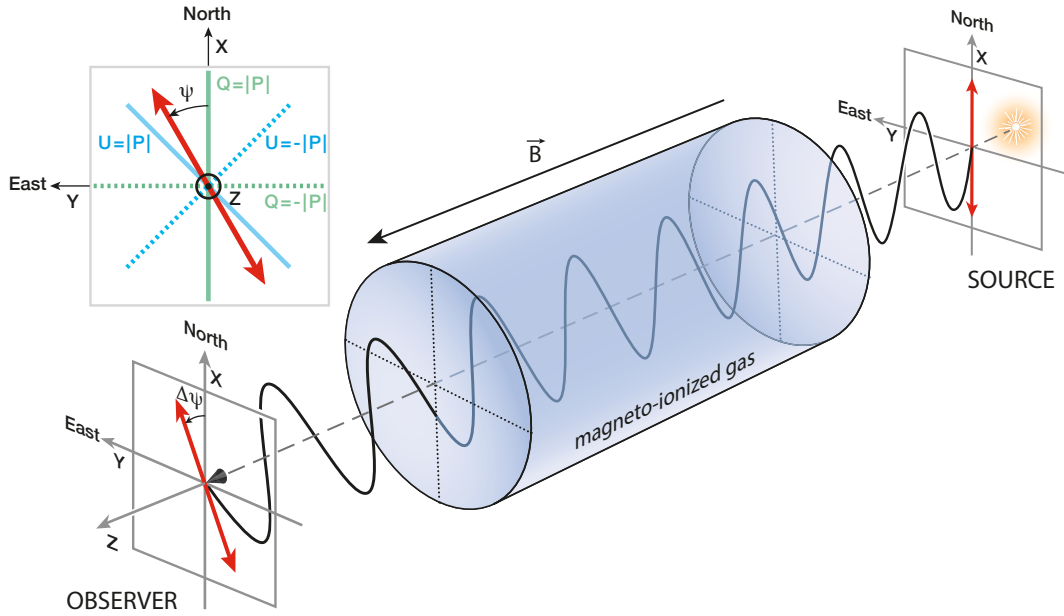


Figure 7: Faraday effect in a magneto-ionized gas, i.e., the ISM within the Milky Way. Note that the polarization of the wave is rotated. You can ignore the green and blue lines labeled  $U$  and  $Q$ . Figure available from [https://upload.wikimedia.org/wikipedia/commons/2/20/Astrophysical\\_Faraday\\_rotation.pdf](https://upload.wikimedia.org/wikipedia/commons/2/20/Astrophysical_Faraday_rotation.pdf)

$$\frac{\text{RM}}{\text{rad m}^{-2}} = 0.812 \int_0^d \frac{n_e}{\text{cm}^{-3}} \frac{B_{\parallel}}{\mu\text{G}} \text{ dl} \quad \text{and} \quad \Delta\Psi_{PA} = \lambda^2 \times \text{RM}. \quad (9)$$

Practically, one has to observe the polarization angle in multiple frequency channels to determine the RM unambiguously. If this is successfully done, one can calculate the average magnetic field strength along the LOS as follows. The integral over  $n_e$  and  $B_{\parallel}$  simplifies to the LOS average of  $B_{\parallel}$  multiplied with the LOS integral of  $n_e$ , which is DM (see Eq. 8.) resulting in

$$\frac{\langle B_{\parallel} \rangle}{\mu\text{G}} = 1.232 \times \frac{\text{RM/rad m}^{-2}}{\text{DM/cm}^{-3}}. \quad (10)$$

#### Key question

What is the Faraday rotation and how does it affect astronomical radio signals? What is the Rotation measure (RM)? What do you need to do to measure it? How can you make use of RM and DM to measure properties of interstellar (magnetized) medium? See also Secs.5.2.5 and 5.3.

**Bonus question**

There are dedicated surveys to search for new pulsars. How does a radio signal have to be processed to find the signature of a pulsar candidate, given what you know about the propagation effects? Which advantages and disadvantages for finding new pulsars exist regarding the selected frequencies for the search?

### 3 Radio interferometry and the LOFAR telescope

#### 3.1 Introductory remarks

In the simplest case, a radio telescope consists of one antenna with a certain directional pattern (and receiving electronics), which means that it is more sensitive to electromagnetic radiation in some directions than compared to other directions. There are many ways to build such an antenna, the most iconic being probably a design where the antenna sits in the primary or secondary focus of a huge dish, which collects radio waves over its full area and focuses them onto the antenna. However, it is often very beneficial to not only have a radio telescope consisting of one antenna, but several of them connected in a way so that the individual signals can be combined (more precisely *correlated*) with each other building a so-called radio interferometer. These telescope arrays achieve higher angular resolution compared to single dishes.

The angular resolution of a (radio) telescope is given by the Rayleigh Criterion

$$\phi_{\text{res}} = 1.22 \frac{\lambda}{D}, \quad (11)$$

where  $\phi_{\text{res}}$  is the resolution of the telescope in units of radians,  $\lambda$  the observed wavelength and  $D$  the diameter of the dish for a single-dish radio telescope, or the diameter of the mirror for an optical telescope.  $\lambda$  and  $D$  are both given in units of meters.

When correlating several antennas to a radio interferometer,  $D$  is defined by the largest *baseline*, where the baseline is the distance between two antennas. Figure 8 illustrates the principle by which radio interferometers work.

Figure 8 uses the most simplistic (though in reality not usable) interferometer, that only consists of two elements. The two dishes have a relative distance  $D$ . A wave front will thus have to travel an additional path  $c\tau_g$  to reach antenna H1, compared to antenna H2. This delay causes a shift in the phase of the detected signal between the two antennas.

This means that by shifting the phases with respect to one another (this is called introducing the *geometric delay*), the radio telescope can be made particularly sensitive towards one arbitrary point in the sky, because the wavefronts from this direction will interfere constructively whereas wavefronts from other locations will tend to cancel out. The location in the sky that corresponds to the strongest constructive interference is called the *phase center*. By adjusting the geometric delay, the phase center can be moved, e.g. to the location of a pulsar.

#### Key question

What is the fundamental principle of radio interferometry? What governs the spatial resolution?

#### 3.2 The LOFAR telescope

The LOw Frequency ARray (LOFAR)<sup>1</sup> is a radio interferometer centered in the Netherlands, designed to explore the frequency range from 30 to 240 MHz. It has two different antenna types, Low Band Antennas (LBA) operating at 30 – 80 MHz and High Band Antennas (HBA) operating at 110 – 240 MHz. Both types are constructed as linear orthogonal dipole antennas.

LOFAR consists of multiple antenna stations, grouped in a core of 30 stations, within which 6 stations form the "superterp" for the shortest baselines (see fig. 10). Additional remote stations are spread across the Netherlands and other European countries. The core stations have  $2 \times 48$  LBAs and  $2 \times 24$  HBA tiles each, the remote stations in the Netherlands consist of  $2 \times 48$  LBAs and one array of 48 HBA tiles and the

<sup>1</sup><https://science.astron.nl/telescopes/lofar/lofar-system-overview/>

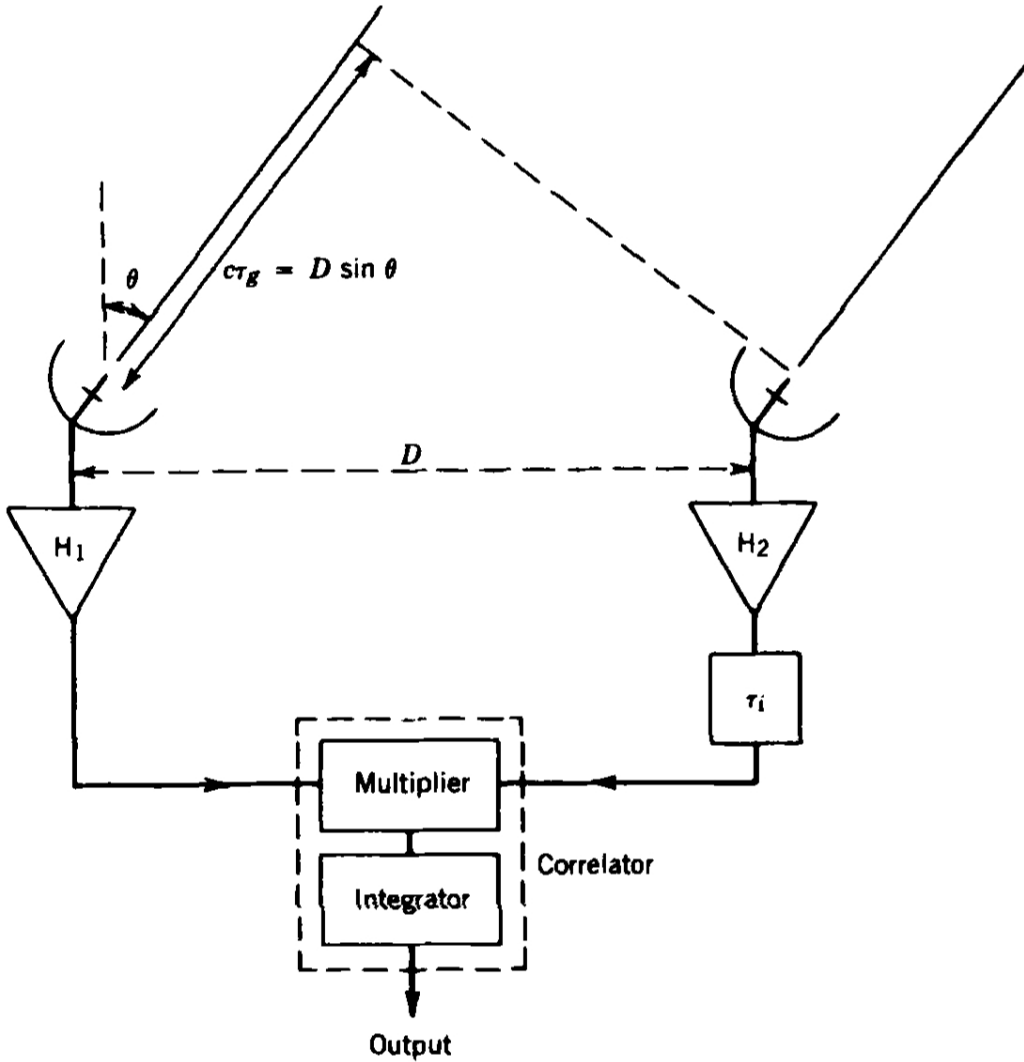


Figure 8: Two antennas centered on the same source with the different pathlengths from source to antenna leading to a relative delay  $c\tau_g = D \sin \theta$  of the radio signal. This delay is compensated for using the instrumental delay  $\tau_i$ .

international remote stations have 96 LBAs and 96 HBA tiles (van Haarlem et al., 2013). The full-width-at-half-maximum (FWHM), and therefore the spatial resolution, of a single international station with the HBAs at 120 MHz, is 2.59 deg.

LOFAR has three major observation modes: interferometric mode, beam-formed modes and direct storage mode (van Haarlem et al., 2013). The interferometric mode is used to get images. The direct storage mode saves the raw data of single antennas for a short time period. The beam-formed modes are used for time-dependent observations, thus also for pulsar observations (Mode 5). For all observations full polarimetry is recorded. The signal is digitized in 195 kHz wide sub-bands, up to 244 can be chosen for a bandwidth of 48 MHz (van Haarlem et al., 2013). The resulting dataset is divided into a number of subintegrations of a given length, which will be seen in the analysis in section 5.2.1.

### Key question

How are pulsars observed with LOFAR? Which observing mode is used and why?

### 3.3 RFI

Radio-frequency interference (RFI) is usually human-made artificial radio signals interfering with the observed data (for instance satellites, power lines, radio and TV stations). Natural sources like lightning or solar activity can also count as RFI. Only a few frequency bands are reserved exclusively for astronomical observations.

In the observation RFI is seen as a distortion in a time series or a frequency band, mostly by excessively high amplitudes (as seen in Figure 12). RFI is often much stronger than the astronomical signal and therefore affected data can only be removed and not corrected. The removal process of the affected data is called flagging. Flagging is explained in section 5.2.2.



Figure 9: Map of central Europe with the individual LOFAR-stations.

#### Bonus question

What are the advantages of using an interferometer for pulsar observations?

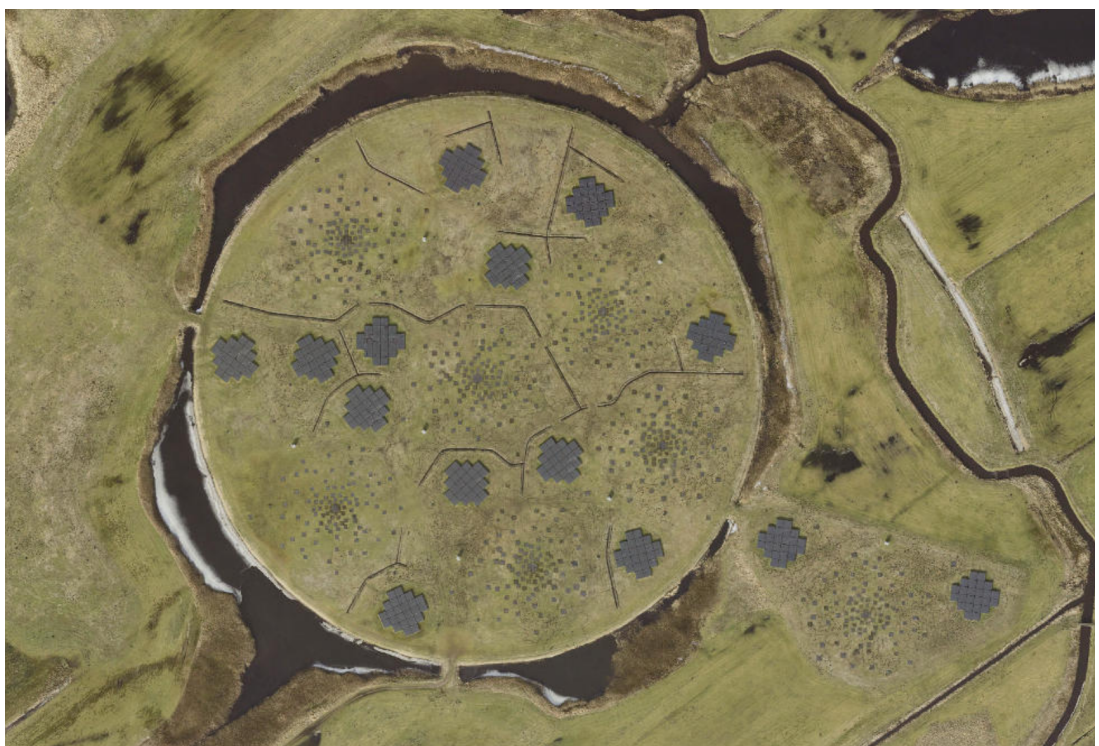


Figure 10: Aerial photograph of the Superterp. The stations seem to be placed rather chaotically, but this is intentional, because having many baselines with different length and orientation increases the image quality. This is generally true for all radio interferometers.

## 4 Choosing your targets

The target selection is based on the Australia Telescope National Facility (ATNF) Pulsar Catalogue. For assistance with the selection process, a Python Jupyter Notebook will be given to you.

It guides you through different steps, starting with a preselection of the catalogue, narrowing it down to sources above or below thresholds for parameters like declination, flux density and dispersion measure. After that you compare properties and select a number of interesting sources, which you then check for their respective observability. The final target list can be exported as an ascii-file.

To properly understand the process of target selection, especially the part where you check the observability, a basic understanding of astronomical coordinate systems is needed.

**Task/Key question:** What coordinate systems are usually used in astronomy? Look for the terms Right Ascension and Declination.

## 5 Analysis

### 5.1 Technical advice

The data you will work with during this lab course is provided to you in the form of a `psrchive`-file, which is a special file format that is used in pulsar astronomy to store time-domain observations. There are special programs which directly act on this file or other files that are produced from it when following the instructions below. You will use these programs within the command line (a.k.a. the terminal) of a server named "jansky" after Karl Guthe Jansky, a famous early radio astronomer. The server is accessible from within the AIRUB network, e.g. via the secure shell (`ssh`) protocol.

Jansky runs Linux and can be used by writing short commands in the "Bash" shell language, which is a programming language that is used for command line environments. It provides a set of commands by which you can navigate through the filesystem, manipulate files and start or terminate other programs on the server. You can find a list of the most common commands in the appendix C. Furthermore, every program has its own set of commands, by which you can specify certain actions, determine the mode of operation or specify the names of other files that should be operated upon.

If you have access to the AIRUB-network, you can log into Jansky with different methods. If you do the lab course at the university, you will probably have access to a Linux computer, so that you can just open the terminal and log in via `ssh` typing

```
ssh -Y pulsar_lab@jansky
```

The password is `pulsar`.

If you connect from outside of the AIRUB, please read Section B and open a terminal on `jansky`.

First of all, create a folder in the home directory (`/home/pulsar_lab`), where you will store your data and `cd` (change directory) into the new folder:

```
mkdir YEAR_MONTH_name1_name2  
cd YEAR_MONTH_name1_name2
```

**IMPORTANT:** Before you can work with the pulsar-related programs, you have to activate the software environment they are installed into by typing

```
conda activate pulsar
```

### 5.2 Working with the data

**IMPORTANT:** save all the plots and pictures that you make, because they will be needed for your protocol. You can do this either by special commands (see below for further instructions) or via screenshots, if the commands do not work for some reason. Be prepared that the processing of the data can take some time, e.g. if the dataset has to be processed heavily to identify offsets of various parameters or to correct for them. However, most of the commands below should execute within less than 20 seconds.

#### 5.2.1 Data inspection

The first step is to have a closer look at various parameters of the dataset without changing anything or creating new files. This is helpful to better understand the observation. In the following, the name of the `psrchive`-file will be represented by `FILE`, meaning e.g. `B0329+54.ar`. Starting with the program `psredit`, get a first overview of the most important parameters. Type

```
psredit FILE
```

After you are done with the next section on "Flagging", please repeat this command and see if anything changes. Think about why something changes or why nothing changes.

You can also let the program output specific parameters or characteristics of the observation. This is done by calling `psredit` and inserting `-c <parameter>` in front of the filename. Please run the below commands and answer the questions for yourself and also in the protocol. If you cannot answer some of the questions right away, just go on with the procedure. It will become clearer when you have gone through the steps in the next chapter on flagging.

```
psredit -c name -c coord FILE
```

What does the output tell you? Can you verify that this is the right source that you identified as candidate for observation?

```
psredit -c nchan -c bw -c freq FILE
```

Please note down the setup of the LOFAR Array that was used for your observation.

```
psredit -c int[1]:period FILE
```

Note down the period of your pulsar. It might not be entirely correct yet due to RFI.

```
psredit -c int[1]:duration -c nbin FILE
```

This informs you about the time resolution of the receiver. Can you verify that it is possible to resolve a periodic signal of the same period as your pulsar? How long does the observation take in total?

For the next step in this section, you do not only retrieve information that is already saved within the `psrchive`-file, but also fit parameters like the dispersion measure to it and alter its content. This is done via the program `pav` and will be repeated later, when (if) you have cleaned up the observation from RFI and applied some corrections to it.

```
pav -DFT FILE
```

This command outputs an average pulse profile, that means it tries to overlay all pulse with the correct pulse phase and The x-axis of the resulting diagram is the "pulse phase", which is the time after the beginning of the pulse divided by the currently best estimate of the pulsar period. The y-axis is the added flux of the respective phase bin. The diagram also shows a "signal-to-noise ratio" (SNR) for the pulsar signal, which is a well-defined measure for the strength of the pulsar signal within a particular observation. It is calculated from the average pulse profile over all frequency channels and requires one to set a noise-level, which means to decide when during the pulse phase the pulse begins and the noise ends. You will observe this more closely while flagging the data.

```
pav -DFT -g "PLOTNAME.png/png" FILE
```

Use this command (adding `-g "PLOTNAME.png/png"` to the orginal `pav` command) to save the pulse profile as a png-file to your working directory. Alternatively, you can take a screenshot. Be sure to save the plots

and pictures you are generating during this lab course somehow, as you will need them for your protocol.

```
pav -GTd FILE
```

This diagram shows the same information as the one above (`pav -DFT FILE`), but for each frequency channel separately. This is why it looks like a heatmap, as the flux per phase bin is colour-coded and all channels are positioned next to each other. There are two labels for the y-axis, because it is possible to identify a channel either by center frequency or by a number. The pulsar emission should be visible as some bright curve in this diagram.

What kind of curve can you see for your pulsar? What does it mean if the curve is a straight vertical line? Which functional shape would it have if it was not straight and why is that?

Which additional features do you see? Can you see straight horizontal lines? If there were some, what would they be?

Depending on how well-corrected the observation already is, it is possible that this plot with separate channels looks differently than the averaged pulse profile over the whole bandwidth. The latter one could for instance be broader in pulse phase-space. Can you see something like this with your pulsar? If yes, what could be the (observational) reason? Is there a way to make both profiles have roughly the same width?

```
pav -YFd FILE
```

This plots a pulse phase-time diagram. If your signal is mostly clean, you should be able to spot the pulsar signal as a rather straight column.

Can you find some horizontal lines in addition to the pulsar signal? Even if you do not, how would they most likely come about? What would it mean if you could not see the signal of the pulsar at all, but instead some rather unstructured brighter or darker lines all over the plot?

### 5.2.2 Flagging

This step is concerned with marking (flagging) the parts of the data which are contaminated by man-made radio signals (radio frequency interference, RFI), so that these parts of the observation are not used to produce plots and calculate parameters of the pulsar or the ISM along the line of sight. It can happen that the observation is almost not affected by RFI, so that you do not need to do any flagging. On the other hand, there can be so much RFI that neither you or the program can see the pulsar before flagging or that the observation is entirely useless. To start the flagging process, type

```
pazi FILE
```

Two windows will open. One shows the integrated pulse profile over all frequencies. The other one (window 1) is used for flagging and at first shows a two-dimensional diagram in which the radio intensity is plotted with the pulse phase on the x-axis and time on the y-axis. If you left-click into this window and then press `f` on the keyboard, you can switch to a diagram with frequency on the y-axis. Flagging is probably easier in this one, as the radio devices on earth often transmit within a very small frequency range. However, you can come back to the plot with time on the y-axis if needed by pressing `t`.

**To zoom into a certain area:** first click with the LEFT mouse button on one channel (or time snippet), then again with the LEFT button on another channel. The diagram in window 1 will then only show the interval between these two channels including them. This can be done repeatedly.

**To flag:** click on one channel (or time snippet) with the LEFT mouse button, then with the RIGHT button on another channel (to flag multiple channels), or click only the RIGHT button (to flag only one channel). All channels that you clicked on AND those in between will be flagged.

**To zoom out totally:** press **r**

**Toggle DM correction:** press **d**

**Undo last command:** press **u**

**To save the flagging information within the psrchive-file:** click on window one with the flagging diagrams and press **s**. You can do this several times while you are flagging the observation, and you must do it when you are done.

After you are done with flagging and have SAVED the flagging information you can stop the program by pressing **q** whilst being in window 1. The window with the integrated pulse profile and the SNR is helpful as well, as it helps you to evaluate your progress while flagging. It is updated as you flag, and if everything goes well the profile should become sharper gradually and the SNR should rise considerably. But this does not happen with every single frequency channel or time snippet that you take out. It can also happen that some signals that not part of the pulsar emission make the pulses appear stronger, but nevertheless they should be removed.

What are the SNRs before and after flagging? What else changes about the pulse profile of your specific observation?

Repeat the plots you have done with **pav** in the steps above. Use exactly the same commands for that. What has changed compared to before flagging?

Also re-run the command

```
psredit FILE
```

There, nothing should have changed. Does this make sense to you? Why might the information be still the same?

Finally, run the commands

```
psrstat -jFTD -c snr FILE  
psrstat -jFTD -c snr FILE.pazi
```

and ask yourself what the resulting numbers mean. What does **FILE.pazi** contain? What have you achieved by flagging?

### 5.2.3 DM correction

When the observation still contains a lot of RFI, it is very well possible that the dispersion measure has not been estimated correctly. It was probably possible to see this in the plots in subchapter 5.2.1, given that the pulsar signal was strong enough. In this part, you will re-do the DM estimation based on the flagged observation. The DM has especially big effects on LOFAR-observations because the observing bands are so low in frequency.

Prepare the file with the flagging information by typing

```
pam -T -e pazi.Tscr FILE.pazi
```

and run the analysis with

```
time pdmp FILE.pazi.Tscr
```

Now you need to make a screenshot of the window that opens after you have run the second command, because there may be no dedicated command for saving the plot with the programs used. You will be shown a "DM offset", in the plots as well as in the terminal, which is the residual dispersion measure found in the file with the flagging information. It equates to the difference between the first estimation of the DM before flagging and the real DM of the pulsar during the observation.

The value has an uncertainty to it, which you should pay very close attention to. When do you think is it a good idea to apply a DM correction like in the next step? Should one do it also if the uncertainty is smaller than the offset found? What does it mean for the observation (and for you) if the correction is zero?

To correct for the DM-offset, run

```
pam -d <value> -e pazi.dm FILE.pazi
```

where <value> is a place-holder for the DM offset you just found, which means e.g. you type 5.273 instead of <value> if the DM offset is 5.273. This command also creates a new psrchiv-file in which the observation is now stored (hopefully!) without any dispersion effects of the ISM.

After the DM correction, run

```
pav -DFT FILE.pazi.dm  
pav -YFd FILE.pazi.dm  
pav -GTd FILE.pazi.dm
```

and have a look at the same plots of the integrated pulse profile, the pulse profiles of the separate frequency channels and the pulse phase-time diagram you have already done for the observation before DM correction. Be sure to use the right file which stores the data with the DM correction applied. Can you spot any differences? If yes, how did they come about and what do they mean? Has your DM-correction been successful?

#### 5.2.4 Period correction

In a similar way to the DM-correction, the period estimate can be corrected if it has been affected by RFI. Run the following commands on the file containing the flagged data:

```
pam -F -e pazi.Fscr FILE.pazi
```

```
time pdmp FILE.pazi.Fscr
```

When you have found the offset (and possibly have taken a screenshot of the plot that appears), think about whether it is sensible to apply the correction or not. Your decision should be guided by the uncertainty mentioned along with the offset!

Apply the correction by typing

```
pam --period <value> -e pazi.per FILE.pazi
```

where <value> is the offset and a new file with corrected period will be created. You can find out if the correction has been successful by querying the new file and the old file about their periods, e.g. with

```
psredit -c name -c int[1]:period FILE and  
psredit -c name -c int[1]:period FILE.pazi.per
```

### 5.2.5 Rotation measure correction

To find the original polarisation angle of the pulsar, you need to also correct for the rotation measure of the ISM. Luckily, the rotation measure is in itself an interesting measurement, which means that you obtain two pieces of information in one step. There are several algorithms implemented within the `rmfit` program of `psrchive`. You will use the simplest one called "brute force", which simply tries a number of different rotation measures in some range and calculates the polarized intensity of the whole signal for each trial. The polarization of a pulsar is reduced by the Faraday effect, because the latter is frequency dependent. Therefore, averaging over all frequency channels of a signal being affected by constant rotation measure, many polarization vectors pointing in different directions are summed up, causing depolarization. This means that the more precisely the vectors are "rerotated" by a negative rotation measure, the higher the polarization of the whole signal will be.

Using the file with the flagging information as a basis, you could utilise the automatic mode by typing

```
rmfit -t -D -K/xs FILE.pazi
```

Typing `-D -K/xs` makes sure that the software not only finds the RM, but also saves a text file with a list of the polarized intensity as per trial RM. Additionally, it creates a plot out of this file, the so-called rotation measure spectrum.

However, if you want to learn a little more, you can set the upper and lower bounds for the trial rotation measures as well as the number of trials by hand. This is done with

```
rmfit -m min_rm,max_rm,num_steps -D -K/xs FILE.pazi
```

where `min_rm` and `max_rm` are the lower and upper bound, respectively, and `num_steps` is the number of trial rotation measures. To decide for proper upper and lower bounds, you can have a look in the ATNF pulsar catalogue and set them in such way that they include the catalogue value for the RM. But do not choose the range to small, because your findings may differ slightly from the catalogue values and `rmfit` should ideally be provided with a full curve of the polarization fraction rising from the noise floor to maximum and back to the noise floor and only a part of it.

For many (but not all!) pulsars, you can just run

```
rmfit -m -100,100,1000 -D -K/xs FILE.pazi
```

Pay attention to the terminal output that is generated by the above commands. It could happen that `rmfit` does not interpret your commands properly, e.g. utilizing automatic mode although you specified the conditions for the trial rotation measures yourself. It is not a desaster if this happens, because the rotation measure will probably be found anyway. In any case you should look at the rotation measure spectrum to determine if your bounds and possibly also the number of rotation measures to be tested were a good choice. If they were, you should see one big and reasonably sharp peak somewhere in the spectrum, but no other conspicuous features.

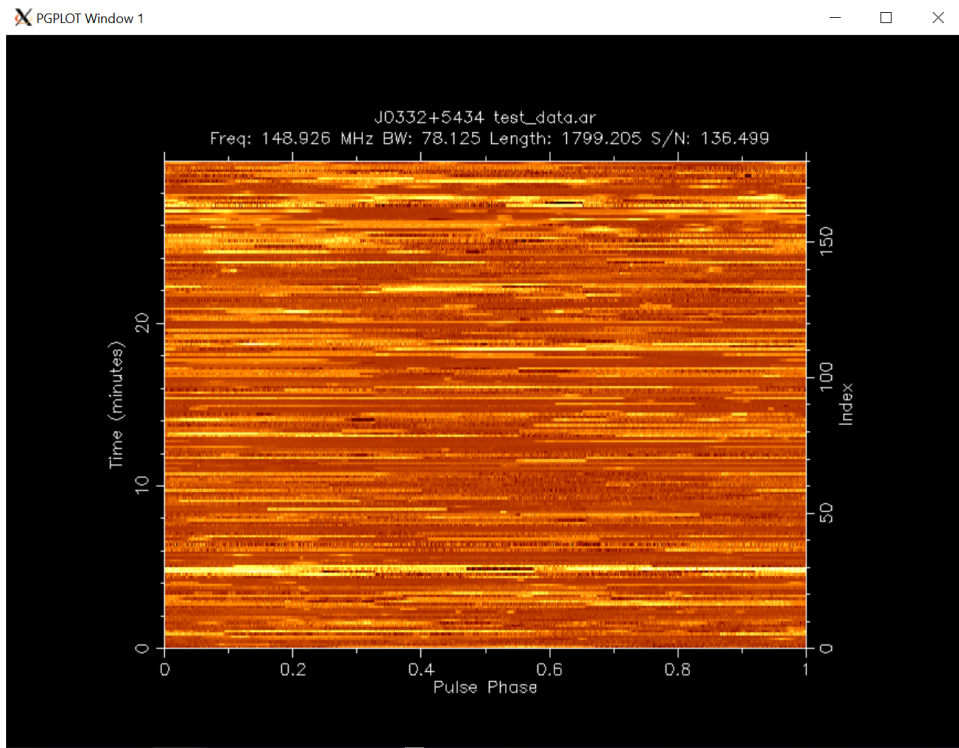


Figure 11: **Flagging:** radio power of an observation displayed with color code depending on pulse phase and time. You can see that flagging might turn difficult in this diagram, since the emission from the pulsar is not even visible.

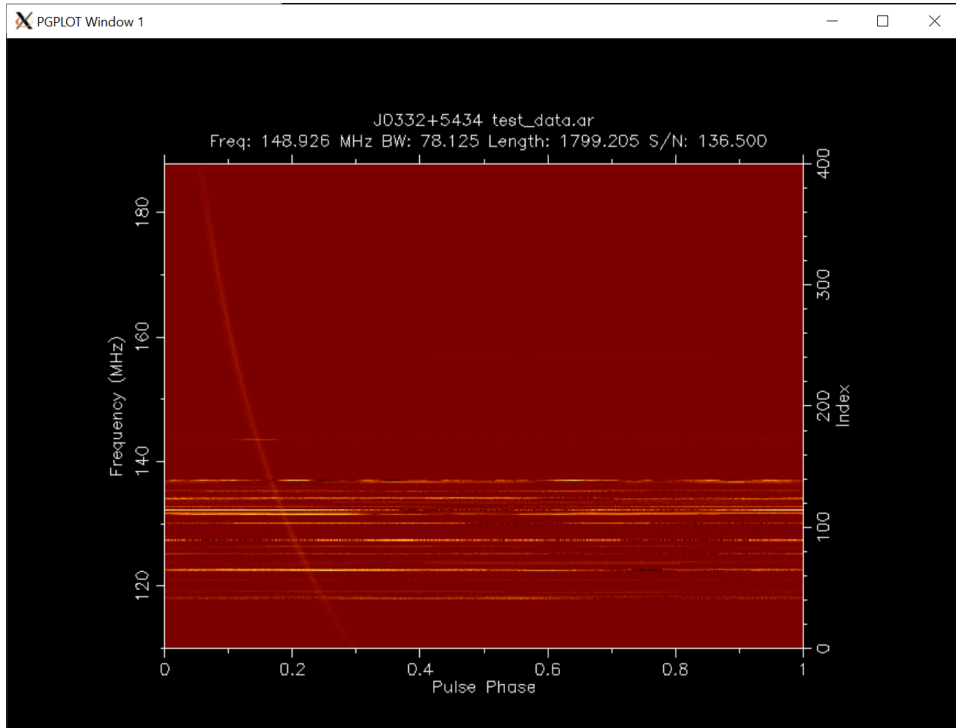


Figure 12: **Flagging:** radio power of an observation displayed with color code depending on pulse phase and frequency, i.e. every frequency channel is folded according to the pulse phase. The faint curved line starting at the top left of the frame is the pulsar signal.

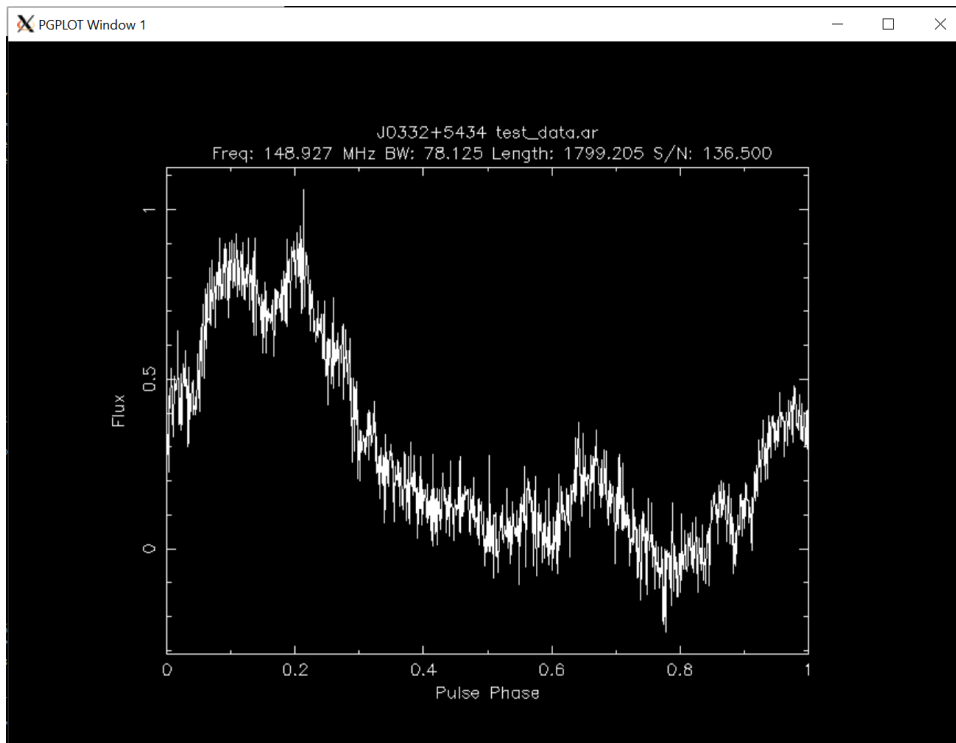


Figure 13: **Flagging:** pulse profile before flagging.

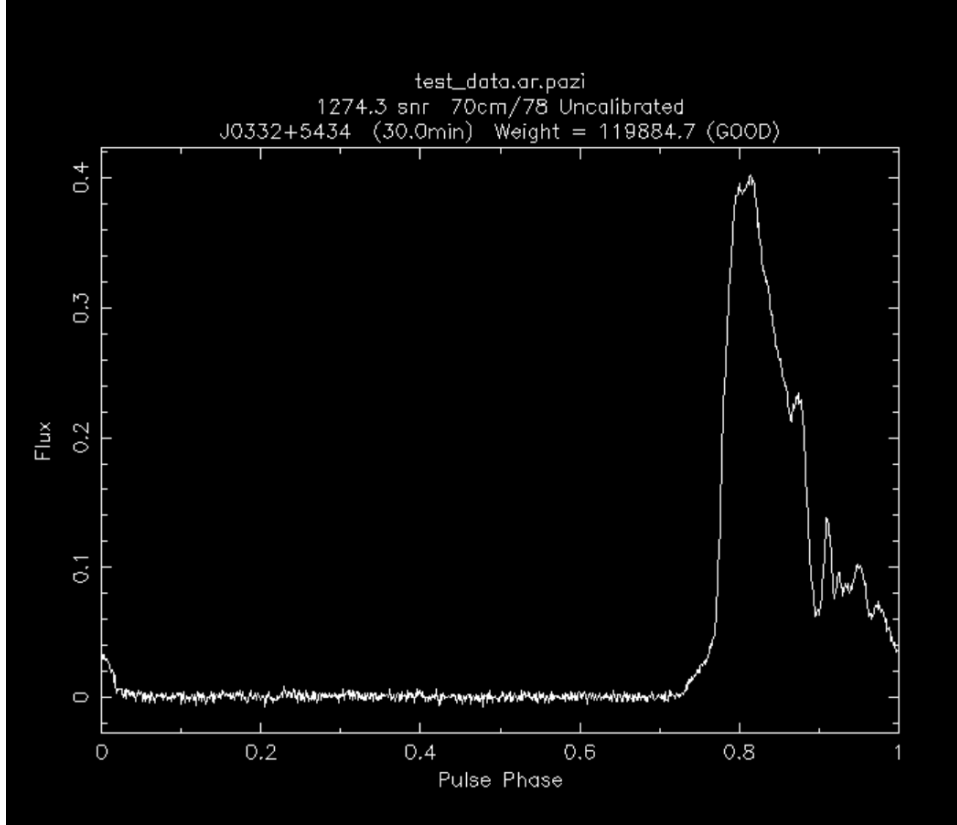


Figure 14: **Flagging:** pulse profile after successful flagging. Note the substantially increased SNR even though to total radio intensity is lower than before.

### 5.3 Galactic magnetic field and distance

As was discussed in sec. 2.4, one can get an estimate for the average magnetic field strength along the line of sight just from knowing the rotation measure and the dispersion measure, because of

$$\frac{\langle B_{||} \rangle}{\mu G} = 1.232 \times \frac{RM/\text{rad m}^{-2}}{DM/\text{cm}^{-3}} \quad (12)$$

**Task:** Calculate  $\langle B_{||} \rangle$  for all pulsars that you observed. Use the uncertainties of RM and DM to obtain an uncertainty for  $\langle B_{||} \rangle$  by Gaussian error propagation. Think about how meaningful this uncertainty might be and discuss it.

Furthermore, it is possible to estimate the distance to pulsar with either RM or DM, provided the average electron density along the line of sight is known. Because using your measurement of RM to calculate the distance would be based on your result for  $\langle B_{||} \rangle$ , which you have obtained knowing DM, you can just calculate the distance with the dispersion measure. Its definition can be rewritten as

$$DM = \int_0^d n_e \, dl =: \bar{n}_e \cdot d \quad (13)$$

with distance  $d$  and the average electron density  $\bar{n}_e$  defined by the left integral.

**Task:** Use all your measurements of DM to estimate the distances to the respective pulsars. If possible, use different, but plausible values for  $\bar{n}_e$ , e.g. general averages for the galactic disk (if the pulsar is in the galactic disk) or more precise values from ISM maps. Compare your results to one another and with literature values. A first starting point for those would be the ATNF pulsar catalogue, where you can find DM based distances for almost all pulsars and distances measured with other techniques for some. Your

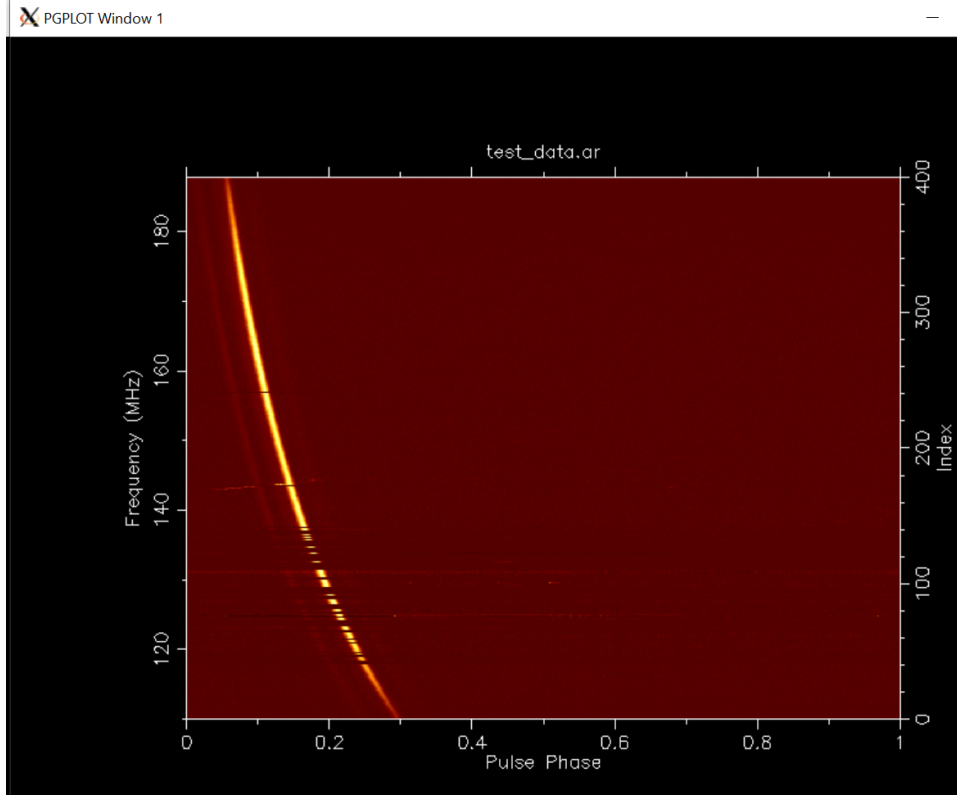


Figure 15: **Flagging:** phase-frequency diagram after flagging. Now, the pulsar signal is the brightest part of the observation. Note that there is still RFI present. It could be removed, but only at the cost of also removing similarly strong parts of the pulsar signal.

supervisor will instruct you further and help you to come up with estimates for  $\bar{n}_e$ . Finally, include the position on the sky to pinpoint the three-dimensional location of every pulsar. Mention in which area of the Milky Way they are located in your protocol. Can you spot some selection effects?

#### 5.4 Pulsar magnetic field and characteristic age

**Task:** Look up the period derivatives  $\dot{P}$  of each of your observed targets in the ATNF pulsar catalogue. Use it together with your measurement of  $P$  to calculate the lower bound for the magnetic field as well as the characteristic age. To get  $B$ , you need to come up with reasonable estimates for the pulsar radius  $R$  and its moment of inertia  $I$ . With the knowledge gathered while working on this lab course, you should be able to estimate  $R$  and  $I$  easily.

Furthermore, plot the pulsars you have observed into a  $P$ - $\dot{P}$  diagram. Ideally, the axes should be scaled logarithmically. To which population does each of them belong? Can you say something about their respective stages of development?

#### 5.5 Special effects

**Task:** Have a close look at fig. 20 and see if you can spot deviations from the usual scheme of regular pulsed emission. Assuming that the data is not corrupted and complete, i.e. you see the full emission of the pulsar in that range of frequency and time and nothing else, think about how the features that you see can be categorized. Have you seen something like this in your pulsar observations? If yes, why do you think your anomalies are not just caused by RFI?

In any case, do some research on your own on exceptions to the regular emission pattern. Sum up your

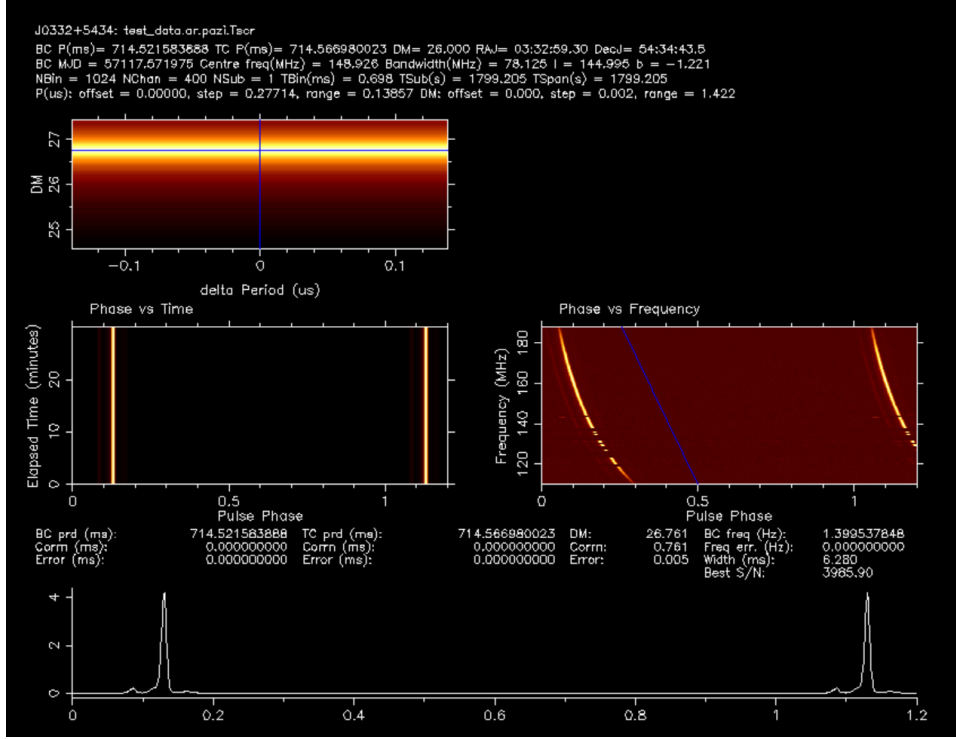


Figure 16: **DM correction:** typical report of the DM correction program after successful flagging. You can see that DM has to be adjusted by  $0.761 \pm 0.005$

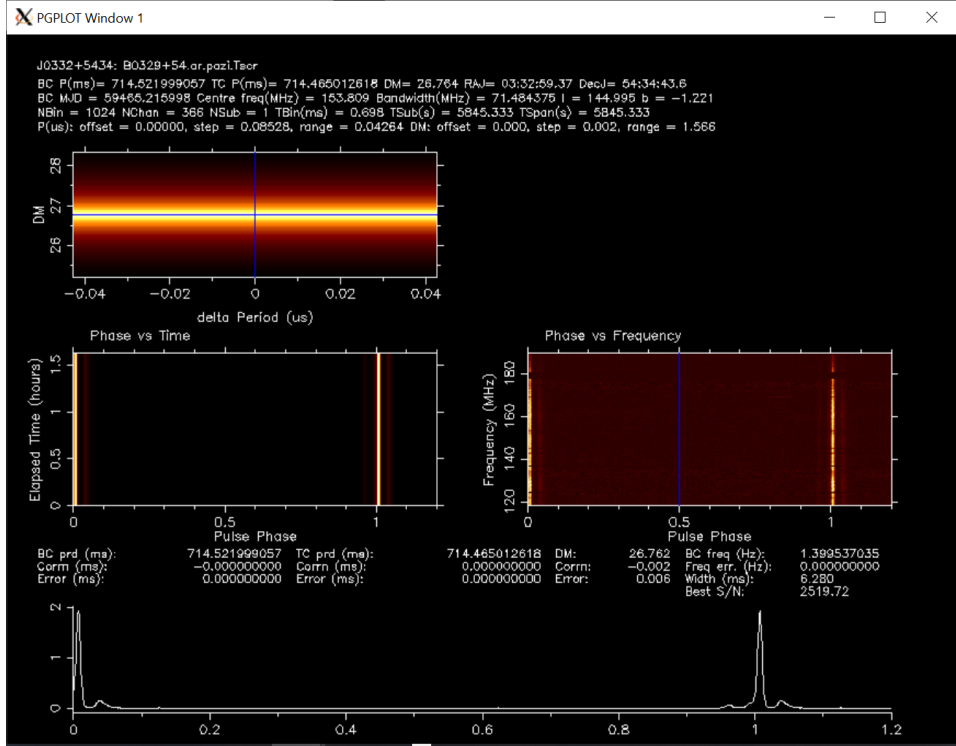


Figure 17: **DM correction or time pdmp:** typical report of the DM correction program when the dispersion measure is correctly estimated. Note that the correction to DM is within its uncertainty.

findings in the protocol and link them to your own observations, if you have seen them. Some useful keywords

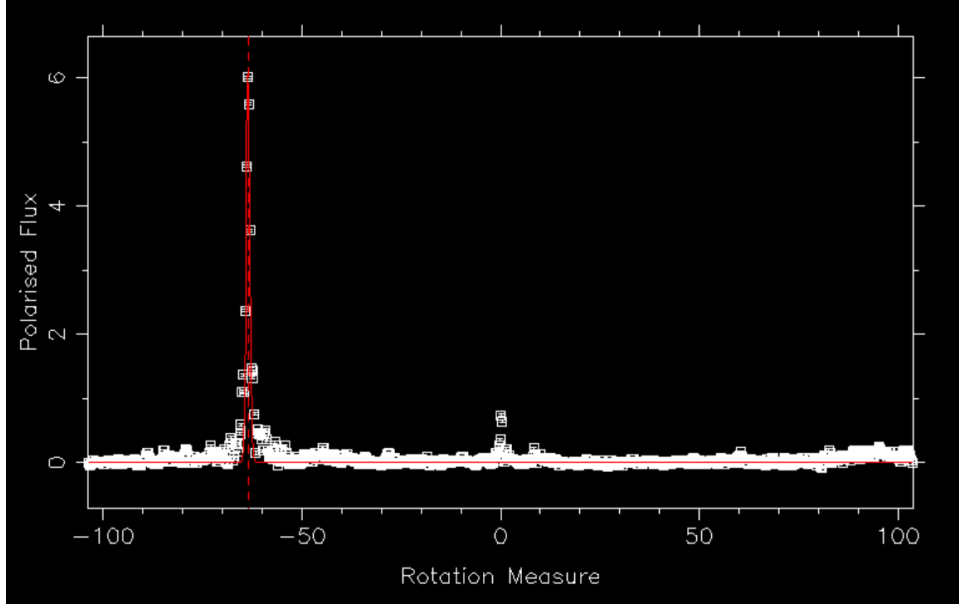


Figure 18: Rotation measure spectrum of pulsar B0329+54 (or J0332+5434) with 100 trials and  $-100 < \text{RM} < 100$ . The best fit RM is  $\text{RM}_{\text{opt}} = -63.58733 \pm 0.03$

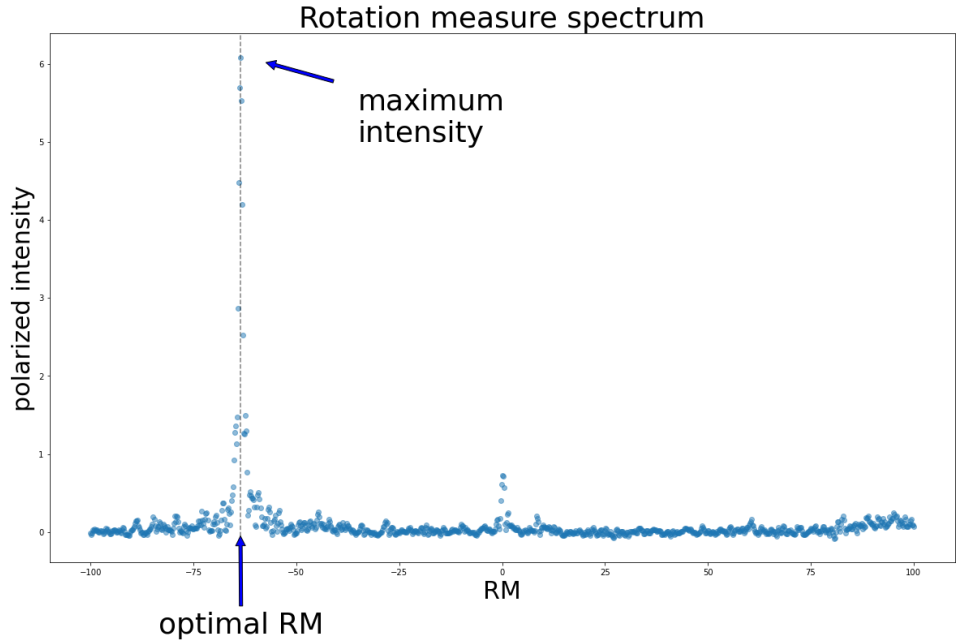


Figure 19: The same as in 5.2.5, but plotted with matplotlib from within Python. With the data plotted here, you could fit the curve yourself and find the rotation measure this way.

could include *nulling*, *drifting sub-pulses*, *glitches* and *mode changing*.

**Solution:** Firstly, it is possible that a radio pulsar suddenly cannot be seen any more, meaning that it misses out on some pulses, but keeping its period and phase when the pulses reappear. This phenomenon is known as *nulling* and can be observed for a large part of the pulsar population. The amount of nulling that one pulsar exhibits ranges from "no evidence for nulling" to the condition that a pulsar is rarely ever visible in radio because it is almost always nulled Lorimer & Kramer (2004).

Nulling is similar to another transition in the behavior of a pulsar that is called *mode changing*. Here, the pulsar suddenly switches to another integrated pulse profile and exhibits it for some time. Usually, one

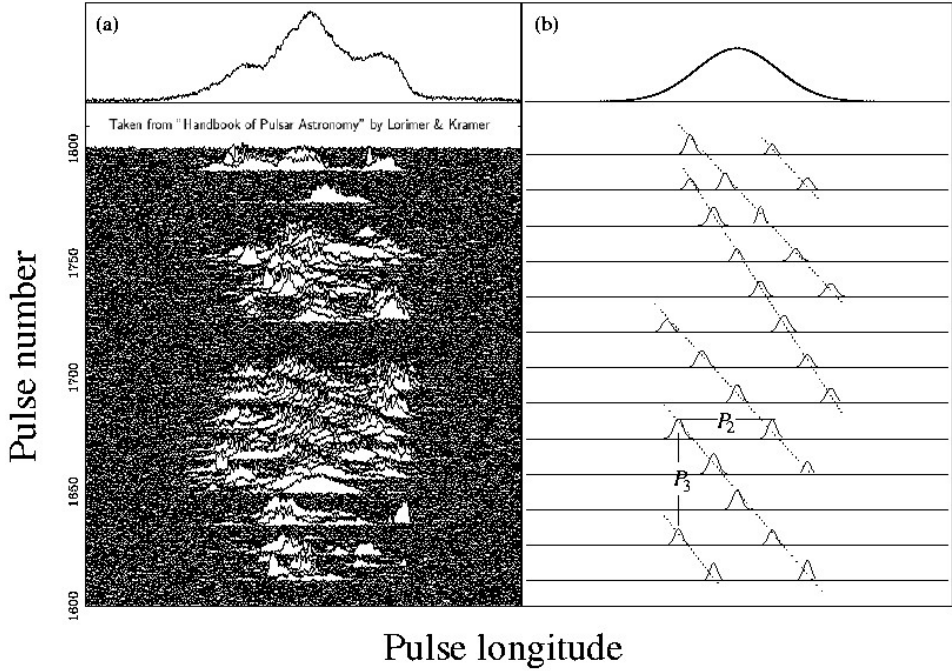


Figure 20: (a) Real data of PSR B1944+17, showing a sequence of many pulses. Nulling can be spotted easily, as well as mode changing. (b) Schematic view of drifting sub-pulses.  $P_2$  is the characteristic spacing of the subpulses,  $P_3$  is the period at which the sub-pulses cross the pulse window. The different slopes indicate different drift rates for each set of drifting pulses.

profile will be favored over the other, which is just sporadically expressed. This phenomenon, as well as nulling and also the next point, is thought to be related to similar highly ordered changes in the interior of the pulsar. Lorimer & Kramer (2004)

Some pulsars also exhibit so-called "drifting sub-pulses", i.e. additional pulses that drift across a pulse window at a fixed rate (but not with the same rate every time). These can come in distinct sets with different periods and fixed time offsets between the sets. One possibility to explain this behavior comes from the idea that there is not only one smooth beam, but a structured one having several sub beams (which is anyway a widely favored concept), and that the drift is created by these beams rotating even with respect to the neutron star surface. Lorimer & Kramer (2004)

Furthermore, there is a type of rotational instabilities known as "glitches", which means that the rotation rate suddenly increases by small value and often exponentially decays back to the conditions before the glitch. For the well-known Vela pulsar, the recovery from a glitch can take several years, but this only becomes apparent if one has already subtracted the overall spindown. While they are generally rare, they are more frequent for some pulsars than for others. It is considered to be likely that glitches are produced by some kind of interaction between the crust and the neutron superfluid under it. Even if the precise mechanism is not known yet, the evidence for a superfluidal interior of neutron stars provided by glitches is considered to be strong. Lorimer & Kramer (2004)

## References

- Antoniadis, J., Freire, P. C. C., Wex, N., et al. 2013, Science, 340
- ATNF Pulsar Catalogue. 2022, Pulsar Catalogue of the Australian National Telescope Facility
- Bell-Burnell, J. 1977, Annals of the New York Academy of Science, 302, 685
- Lattimer, J. M. 2021, Annual Review of Nuclear and Particle Science, 71
- Lorimer, D. R. & Kramer, M. 2004, Handbook of Pulsar Astronomy (Cambridge University Press), A312
- Manchester, R. N., Hobbs, G. B., Teoh, A., & Hobbs, M. 2005, Astronomical Journal, 129, 1993
- The Fermi LAT Collaboration. 2015, Science, 350, 801
- van Haarlem, M. P., Wise, M. W., Gunst, A. W., et al. 2013, Astronomy Astrophysics, 556, A2
- Wilson, T. L., Rohlfs, K., & Hüttemeister, S. 2013, Tools of Radio Astronomy
- Zolotukhin, I. Y., Bachetti, M., Sartore, N., Chilingarian, I. V., & Webb, N. 2016, The Astrophysical Journal, 839

## A Famous pulsars

To familiarize yourself more with the astronomical objects that you will study in this lab course, you are invited to ingest the following list of pulsars (and neutron stars) which have made their way to fame. Your supervisor will probably be kind enough not to demand detailed knowledge about the content of this section.

- **LGM-1:** the first object identified as a pulsar. Called in modern terms PSR J1921+2153 or PSR B1919+21 and nicknamed "Little Green Man-1" as an allusion to extraterrestrial intelligence, it spins with a period of roughly 1.338 s and is only 300 pc away from the earth (not measured via the dispersion measure) Manchester et al. (2005).
- **The Crab pulsar:** having been detected in 1968, this pulsar with the identification PSR B0531+21 was very important in establishing a link between neutron stars and pulsating radio sources. This is because the neutron star at the center of the Crab nebula can actually be observed pulsing in the optical Wilson et al. (2013), indicating that the pulsed radio emission is from the same source. Wilson et al. (2013)
- **The Hulse-Taylor pulsar:** the first binary system with a pulsar (and a non-pulsing neutron star), PSR B1913+16, was discovered with the Arecibo-Telescope by Robert Allan Hulse and Joseph Hooton Taylor. Through pulsar timing, it was soon found that the pulsar was in a binary system and had an orbital period of 7.75 hours. When observing the system repeatedly over several years (decades until now), the change of the size of the orbit could be measured, fitting together almost perfectly with the prediction of energy-loss through gravitational waves. This is known as the first indirect detection of gravitational waves, which earned Hulse and Taylor a nobel prize in 1993. Lorimer & Kramer (2004)
- **The first double-pulsar:** J0737-3039 consists of a 22.7 ms pulsar in orbit around a 2.77 s pulsar. This double-pulsar configuration increases the precision of orbital measurements (and therefore strong-field gravitational measurements) over a system like the Hulse-Taylor pulsar, where the other neutron star does not pulse. Lorimer & Kramer (2004)
- **The first pulsar planetary system:** Two earth-mass planets and one of lunar-mass were found orbiting the pulsar B1257+12 in 1990 (publications 1991, 1994) and where discovered with the Arecibo telescope. This was the first discovery of an exoplanetary system! Lorimer & Kramer (2004)
- **Geminga:** the first pulsating  $\gamma$ - and x-ray source which is almost invisible in the radio regime has been discovered in 1975. Objects like this, which show all the signs of a rotation-powered pulsar in the high-energy emission, but are not really visible, challenged the definition of the word "pulsar" from being merely observational to be based onto the physical phenomenon of a rotating neutron star. At last, it could well be that Geminga and similar sources have either low intrinsic radio luminosity or the radio beam is e.g. narrower than the one of the high-energy emission and simply does not point along the line of sight. Lorimer & Kramer (2004)
- **GW170817:** the first-observed gravitational wave event originating from a binary neutron star merger was detected by the aLIGO-observatory in 2017 (black hole mergers were detected before that). Although the two neutron stars involved have probably not been pulsars anymore at the time of the merger, the event is interesting as it is a true multi-messenger event, which was first seen by aLIGO as a neutron star-merger and by the Fermi satellite as a short gamma ray burst (GRB). In addition, many other instruments performed follow-up observations. From the perspective of astrophysics, the event is also significant because it **a**) yields evidence that short gamma ray bursts are indeed produced by neutron star mergers, and **b**) that neutron star mergers can produce heavy elements (e.g. gold, platinum) as it had been proposed before.

## B Remote access

As this lab course mostly relies on working with data on a server, it is possible to work on it from home. There are three requirements for this: first, one needs access to the internal network of AIRUB. This is achieved with a VPN-connection, and the system administrator will give you time-limited VPN keys for this. Second, one needs a program which establishes the connection to the server and gives access to its terminal. Generally, this can be done from the command line of one's computer and one can just use one's own terminal and `ssh` if one runs Linux. Thirdly, a remote connection with graphical input and output is necessary to display the many diagrams (see the sections to follow) and to click on frequency channels and/or time snippets when flagging the parts of the data that is contaminated with RFI. The last point is not a concern when one connects from the terminal of a Linux machine, it simply works. However, for Windows, one requires a feature called "X-11 forwarding" and some more specialized software, which will be described in the following.

### B.1 VPN Connection

At the astronomical institute, Windows users tend to use "OpenVPN GUI". Three files will be provided by the system administrator. They will be named something like `your_name`, `your_name-TO-IPFire` and `ta`. All one needs to do is to copy them into the folder that OpenVPN has created for its configuration files. The path should be similar to `C:\Users\your_name\OpenVPN\config`. Alternatively, you can right-click onto the OpenVPN symbol in the activity tray and then import the files.

More information about OpenVPN on Windows can be found here: <https://www.ovpn.com/en/guides/windows-openvpn-gui>.

### B.2 GUI-Access

#### B.2.1 X2GOClient

**When accessing jansky from out side of the institute, we recommend to use the X2GoClient.** Download the client from: <https://wiki.x2go.org/doku.php/download:start> and install it on your computer. Start the program and create a new session (Sitzung → Neue Sitzung). You just need to enter the following details:

- Host: `jansky.shadow2.airub.net`
- Login: `pulsar_lab`

You further need to select CINNAMON as your desktop environment in the drop down menu "Sitzungsart".

#### B.2.2 PuTTY and X-11 forwarding

You can also use the program PuTTY (<https://putty.org/>) for the connection and the program Xming (<https://sourceforge.net/projects/xming/> or <https://xming.en.softonic.com/>). PuTTY just allows to login on the server with a terminal, it has no graphical interface itself. The graphical interface can be enabled by using Xming. After installing both, one has to start Xming by clicking on its icon. However, it will run in the background and will only display an icon in the activity tray, but not a dedicated window. Then, one opens PuTTY to set up the connection. Before connecting, it is required to go to **Connection → SSH → X11** and set a check mark with the option "**Enable X11 forwarding**". Only then one will be able to see the plots from the pulsar software and to flag the data.

Finally, one goes back the **Session** part of the configuration panel to enter as host name `pulsar_lab@jansky`. Lastly, one clicks **Open** and the terminal of the server should appear, asking for the password (see the above section).

## C Linux terminal commands

Command	Explanation
command [options] [arguments]	general structure of a command. Options are often typed with dashes, -[option], arguments will often be filenames.
ssh user@host ssh -Y pulsar_lab@jansky	Log into a server via ssh (secure shell) Log into the server on which the pulsar software is running. Password is pulsar.
logout	logout from a server
cd cd <path>	jump to home directory change directory to a location specified by <path>. This is relative to the current working directory, so you can navigate your way through the directories level by level.
ls (without argument) or ls -l  . / ../	list all files in working directory; -l: include details jump to current working directory jump one directory higher
cp FILE1 FILE2	copy FILE1 to FILE2, FILE2 being the new filename
cp FILE1 <path>	copy FILE1 to <path>. Make sure you provide the correct path!
cp FILE1 <path> -r	copy FILE1 to new <path>. Make sure you provide the correct path!
rm [argument] rmdir [argument] rm -r [argument]	remove (delete) a file provided as an argument remove an empty directory remove a non-empty directory
nano FILE vim FILE	open FILE in nano text editor open FILE in vim text editor
↑	Show the last commands. You can press it several times.
Cmd + c	Abort the command currently running. Cmd is Strg on German keyboards.
Cmd + z	Pause the command currently running
fg	Continue command
bg	Continue command in the background
Cmd + u	Delete the current line
killall [process]	End all programs with name process
Command	Explanation
export VARNAME=file.txt	setting a variable VARNAME to reference file.txt in the terminal. This is handy for your pulsar data archives!
[command] \$VARNAME	To use a variable with a command, you have to write a \$-sign in front of it.